NIH Public Access
Author Manuscript
Hippocampus. Author manuscript; available in PMC 2012 June 18.

Published in final edited form as:
Hippocampus. 2008 ; 18(7): 668–678. doi:10.1002/hipo.20426.

Altered Morphology of Hippocampal Dentate Granule Cell Presynaptic and Postsynaptic Terminals Following Conditional Deletion of TrkB

Steve C. Danzer[1,2,3], **Robert J. Kotloski**[4], **Cynthia Walter**[1], **Maya Hughes**[4], and **James O. McNamara**[4,5,6,*]

[1]Department of Anesthesia, Cincinnati Children's Hospital Medical Center, Cincinnati, Ohio

[2]Department of Anesthesia, University of Cincinnati, Cincinnati, Ohio

[3]Department of Pediatrics, University of Cincinnati, Cincinnati, Ohio

[4]Department of Neurobiology, Duke University Medical Center, Durham, North Carolina

[5]Department of Medicine, Duke University Medical Center, Durham, North Carolina

[6]Department of Pharmacology and Cancer Biology, Duke University Medical Center, Durham, North Carolina

Abstract

Dentate granule cells play a critical role in the function of the entorhinal-hippocampal circuitry in health and disease. Dentate granule cells are situated to regulate the flow of information into the hippocampus, a structure required for normal learning and memory. Correspondingly, impaired granule cell function leads to memory deficits, and, interestingly, altered granule cell connectivity may contribute to the hyperexcitability of limbic epilepsy. It is important, therefore, to understand the molecular determinants of synaptic connectivity of these neurons. Brain-derived neurotrophic factor and its receptor TrkB are expressed at high levels in the dentate gyrus (DG) of the hippocampus, and are implicated in regulating neuronal development, neuronal plasticity, learning, and the development of epilepsy. Whether and how TrkB regulates granule cell structure, however, is incompletely understood. To begin to elucidate the role of TrkB in regulating granule cell morphology, here we examine conditional TrkB knockout mice crossed to mice expressing green fluorescent protein in subsets of dentate granule cells. In stratum lucidum, where granule cell mossy fiber axons project, the density of giant mossy fiber boutons was unchanged, suggesting similar output to CA3 pyramidal cell targets. However, filopodial extensions of giant boutons, which contact inhibitory interneurons, were increased in number in TrkB knockout mice relative to wildtype controls, predicting enhanced feedforward inhibition of CA3 pyramidal cells. In knockout animals, dentate granule cells possessed fewer primary dendrites and enlarged dendritic spines, indicative of disrupted excitatory synaptic input to the granule cells. Together, these findings demonstrate that TrkB is required for development and/or maintenance of normal synaptic connectivity of the granule cells, thereby implying an important role for TrkB in the function of the granule cells and hippocampal circuitry.

© 2008 Wiley-Liss, Inc.

*Correspondence to: Dr. James O. McNamara, 401 Bryan Research Building, Durham, NC 27705, USA. jmc@neuro.duke.edu.
Maya Hughes is currently at Columbia University, Department of Medicine, New York, New York.

NIH-PA Author Manuscript
NIH-PA Author Manuscript
NIH-PA Author Manuscript

NIH-PA Author Manuscript

NIH-PA Author Manuscript

NIH-PA Author Manuscript

Keywords

neurotrophin; BDNF; epilepsy; DG; synaptic plasticity

INTRODUCTION

Hippocampal dentate granule cells have polarized morphologies, with dendrites projecting from the apex of the cell body into the dentate molecular layer and axons projecting from the basal pole into the dentate hilus and CA3 pyramidal cell layer. Excitatory afferents to granule cell dendrites in the molecular layer are organized into three distinct lamellae. The layer two cells of lateral and medial entorhinal cortex (EC) project to the outer and middle thirds of the granule cell dendritic tree, respectively, whereas excitatory synaptic inputs to the inner third of the granule cell dendritic tree are derived principally from associational-commissural afferents. Granule cell axons, called mossy fibers, are equally complex. Mossy fiber axons exhibit three distinct presynaptic terminal specializations, giant mossy fiber boutons, filopodial extensions of these boutons, and *en passant* terminals. These terminals have distinct synaptic partners. Giant mossy fiber boutons contact and excite glutamatergic CA3 pyramidal cells, while *en passant* and filopodial terminals excite GABAergic inhibitory interneurons. These inhibitory neurons constitute the primary efferent target of granule cells and provide feedforward inhibition to CA3 pyramidal cells (Frotscher, 1989; Acsády et al., 1998; Seress et al., 2001). Feedforward inhibition of pyramidal cells is likely critical for normal hippocampal function, as granule cell—CA3 pyramidal cell synapses are extremely robust, because trains of action potentials in a single granule cell are sufficient to fire its target CA3 pyramidal cell (Henze et al., 2002). Feedforward inhibition of pyramidal cells provides a mechanism to keep this powerful synapse in check. Correspondingly, disruptions in the connectivity of dentate granule cells are thought to play a key role in the development of limbic epilepsy.

Brain-derived neurotrophic factor (BDNF) and its receptor TrkB are important regulators of granule cell morphology. Both molecules are expressed at high levels by granule cells, and BDNF protein is concentrated in the inner and middle molecular layers of the DG (Conner et al., 1997; Danzer et al., 2004a). Moreover, BDNF protein is localized to all three presynaptic terminal specializations of granule cells (Danzer and McNamara, 2004). Functionally, BDNF modulates synaptic inhibition (Olofsdotter et al., 2000) and plasticity (Messaoudi et al., 1998; Asztely et al., 2000; reviewed by Bramham and Messaoudi, 2005) of neocortical—granule cell synapses and is required for long-term potentiation of the granule cell—CA3 pyramidal cell synapses (Huang et al., in press). BDNF and TrkB also play important roles in the development of epilepsy (reviewed by Binder and Scharfman, 2004). In tissue from humans with epilepsy, BDNF mRNA and protein levels are increased (Mathern et al., 1997; Takahashi et al., 1999; Murray et al., 2000) and addition of BDNF enhances excitability in tissue from epileptic animals (Scharfman et al., 1999) and humans (Zhu and Roper, 2001). During epileptogenesis, BDNF protein levels are increased in granule cell pre-synaptic terminals (Danzer and McNamara, 2004) and TrkB receptors are activated in the mossy fiber pathway in multiple models of limbic epileptogenesis (Binder et al., 1999; He et al., 2002; Danzer et al., 2004b). Transgenic overexpression of BDNF sensitizes mice to chemoconvulsant-induced status epilepticus (Croll et al., 1999; Lähteinen et al., 2003) and reduced expression of BDNF impairs epileptogenesis (Kokaia et al., 1995; He et al., 2004). Similarly, overexpression of truncated TrkB, which acts as a dominant negative receptor of BDNF, reduces epileptogenesis (Lähteinen et al., 2002). Finally, in the conditional TrkB knockout line utilized for the present study, kindling epileptogenesis was completely blocked (He et al., 2004).

NIH-PA Author Manuscript

NIH-PA Author Manuscript

NIH-PA Author Manuscript

Together, these data indicate that BDNF and TrkB are important regulators of granule cell function and that under pathological conditions regulation by these molecules may promote the development of epilepsy. Given the almost ubiquitous presence of these molecules at all types of granule cell inputs and outputs, however, the net effect of TrkB is unclear. To gain insight into this question, we examined granule cell morphology in conditional TrkB knockout mice by crossing these animals to mice expressing GFP in dentate granule cells. Synaptic inputs were assessed by examining dendritic structure and dendritic spines in the inner, middle, and outer molecular layers. Synaptic outputs were assessed by examining giant mossy fiber boutons and giant mossy fiber bouton filopodia. These data provide insight into how TrkB regulates the structure of synaptic inputs and outputs of hippocampal dentate granule cells.

MATERIALS AND METHODS

All procedures conformed to NIH and Institutional guidelines for the care and use of animals. All analyses were conducted with the researcher blinded to genotype and treatment group.

Thy 1 GFP-Expressing Mice

Thy 1 green fluorescent protein (GFP)-expressing mice from the M line were maintained on a C57/B6 background (Feng et al., 2000). The Thy 1 promoter belongs to the immunoglobulin superfamily and drives expression in many neuronal as well as some non-neuronal cells (Feng et al., 2000; Danzer and McNamara, 2004; Walter et al., 2007). Importantly, the dentate granule cells labeled by GFP in our study appear to represent typical granule cells, in that their somatic, dendritic, and axonal architectures replicate patterns revealed by other techniques (Cajal, 1911).

Thy 1 GFP-Expressing Conditional TrkB Knockout Mice

As specified below, symbols in parentheses following genotype specify presence (+) or absence (−) of the TrkB allele. TrkB mutant mice were generated with Cre/lox P technology (Gu et al., 1994) as described previously (Zhu et al., 2001; He et al., 2004). In these animals, the first coding exon of the TrkB gene, which encodes the signal peptide and the first 40 amino acids of the N terminus of TrkB, was flanked by two lox P sites (“floxed”). Crossing these $TrkB^{flox/flox}$ (+/+) mice to transgenic mice expressing cre recombinase driven by the synapsin 1 promoter (synapsin cre positive, +/+) generated progeny in which expression of the floxed gene was selectively eliminated in many CNS neurons (synapsin cre positive $TrkB^{flox/flox}$ [−/−]). Full length TrkB expression in these animals is reduced in neurons within neocortex, pyriform cortex, amygdala, thalamus, hypothalamus and brainstem; in the hippocampus, full length TrkB expression is reduced in CA1 and is undetectable in CA3 and DG (He et al., 2004). Consistent with this pattern, crossing the synapsin cre mice to the Rosa-26 reporter line revealed cre recombinase activity in the overwhelming majority of dentate granule cells. Finally, although recombination is expected to eliminate both full length and truncated TrkB isoforms, minimal reductions of truncated TrkB levels were detected in dentate and CA3 regions of $TrkB^{-/-}$ mice (He et al., 2004). This presumably reflects the fact that truncated TrkB is expressed primarily by non-neuronal cells, which are not targeted by synapsincre driven recombination.

To generate the mice for the present study, synapsin cre negative, $TrkB^{wt/flox}$ (+/+) mice on a 129/C57/ICR background were crossed to Thy 1 GFP-expressing mice on a C57/B6 background to generate GFP-expressing, synapsin cre negative, $TrkB^{wt/flox}$ (+/+) offspring. The F1 generation from this cross was bred to synapsin cre positive, $TrkB^{wt/flox}$ (+/−) animals on the 129/C57/ICR background to generate the offspring used for experiments.

NIH-PA Author Manuscript

NIH-PA Author Manuscript

NIH-PA Author Manuscript

With this design, all GFP-expressing offspring are hemizygous for the Thy1 GFP transgene. Six synapsin cre positive $TrkB^{flox/flox}$ (−/−) mice, four synapsin cre positive $TrkB^{wt/wt}$ (+/+) mice, three synapsin cre negative $TrkB^{wt/wt}$ (+/+) mice, and four synapsin cre negative $TrkB^{flox/flox}$ (+/+) mice were used. Hereafter, synapsin cre positive $TrkB^{flox/flox}$ (−/−) mice will be referred to as $TrkB^{-/-}$, and all other genotypes (possessing both TrkB alleles) will be referred to as $TrkB^{+/+}$.

At two months of age, mice were overdosed with pentobarbital (100 mg/kg) and perfused through the ascending aorta with 4% paraformaldehyde with 1 U/ml heparin in phosphate buffered saline (PBS) (pH 7.4). Forty μm sagittal sections were cut on a cryostat and processed with rabbit polyclonal anti-GFP (1:1000; Chemicon) and goat Alexa Fluor 488 antirabbit antibodies (1:750; Molecular Probes). For each TrkB null mouse, littermate controls were processed simultaneously in the same reaction dishes to assure similar immunostaining in all genotypes.

Fluoro-Jade B Staining

Fluoro-Jade B (Histo-Chem Inc., Jefferson, AR) staining was conducted according to established procedures (Schmued et al., 1997). Sections from animals treated with pilocarpine, to induce status epilepticus and neuronal death, were included as positive controls. Fluoro-Jade B staining of the positive control sections showed extensive labeling of hippocampal and cortical neurons (Fig. 1, lower panel), confirming the efficacy of the protocol. Sections were analyzed using a Leica DMIRE2 inverted microscope equipped with a 63X oil immersion objective (NA 1.4). The number of Fluoro-Jade B positive neurons was determined in the DG for $TrkB^{-/-}$ and $TrkB^{+/+}$ mice. Cell counts were made from four sections per animal.

Anatomical Measures

The following general guidelines were used for all image collection and analysis. Only granule cells brightly labeled with GFP were selected for analysis. GFP-expressing dentate granule cells were imaged using a Leica TCS SL confocal microscope set up on a Leica DMIRE2 inverted microscope equipped with epifluorescent illumination and a 63X oil immersion objective (NA 1.4). Using this system, 3D Z-series stacks were captured at 0.2 μm increments with the pinhole set to 1 Airy unit. Images were captured using 1–6X optical zoom. Quantitative measurements of confocal z-series stacks were made using the Metamorph Imaging system (Universal Imaging Corporation, West Chester, PA, version 4.5r6) or the Neurolucida system (Microbrightfield, Williston, VT). No corrections were made for tissue shrinkage during processing, so size measurements are expected to underestimate in vivo values.

The hippocampal DG contains a heterogeneous population of neurons. This heterogeneity likely reflects differences in function among granule cells, but is manifest in part by position-dependent variability in morphology (Desmond and Levy, 1985; Green and Juraska, 1985; Claiborne et al., 1990). In the present study, we have attempted to account for this variability by examining positionally defined granule cell sub-populations. Even so, it was not always possible to examine the same subpopulation for a given measure. Tracing mossy fiber axons measured in stratum lucidum back to a cell body in the superior or inferior blade, for example, is impractical with the present approach. For the present study, however, we were able to focus our analyses on four subpopulations of granule cells; (1) granule cells located in the outermost region of the superior blade (granule cell-molecular layer border or within one cell body of the border; for example see Figure 2, arrow); (2) granule cells located along the innermost region of the superior blade (granule cellhilar border; for example see Fig. 2, arrowhead); (3) granule cells located throughout the superior

NIH-PA Author Manuscript

NIH-PA Author Manuscript

NIH-PA Author Manuscript

blade (Fig. 2, S); and (4) granule cells from the entire population at the septotemporal level examined. All neurons in the study were from the same septotemporal level (Fig. 2; corresponding to Fig. 113 of Paxinos and Franklin's *The Mouse Brain*, 2001). Subpopulations 1 and 2 reflect the oldest and youngest granule cells, respectively, based on their migration patterns (Altman and Das, 1965; Altman and Bayer, 1990), and were examined separately for analyses of primary dendrite number. Subpopulation 1 was also used for measures of spine density for inner molecular layer dendrites, while dendritic spine densities in the middle and outer molecular layers were obtained from subpopulation 3. Finally, mossy fiber axon measurements and soma profile area measurements reflect granule cells from subpopulation 4. Naturally, our conclusions are limited to the granule cell subpopulations examined, and are not necessarily generalizable to other subpopulations or septotemporal levels.

Soma Area

Soma profile area was measured from confocal images collected using 1X optical zoom. Image stacks were imported into Neurolucida software for quantification. A minimum of 10 neurons per animal were quantified.

Mossy Fibers

Mossy fiber axons of dentate granule cells were imaged in stratum lucidum of CA3b (as defined by Lorente de Nó, 1934; this region also corresponds to the midportion of CA3 which is bounded by the tips of the blades of the DG proximally and the edge of the fimbria distally, Ishizuka et al., 1995). Images for mossy fiber bouton analysis were collected from the center of CA3b (see Fig. 2, box 4), and only suprapyramidal mossy fiber boutons were examined—boutons within or below (infra-pyramidal) the pyramidal cell layer were excluded. Giant mossy fiber boutons were defined as having a cross sectional area of 4 μm^2 or greater (Claiborne et al., 1986; Acsády et al., 1998). Electron microscopy studies have demonstrated that expansions with an area less than 4 μm^2 are either *en passant* terminals, accumulations of mitochondria, or tissue artifacts. *En passant* terminals are functionally distinct since they contact inhibitory interneurons rather than the CA3 pyramidal cells targeted by giant mossy fiber boutons (Acsády et al., 1998); however, given the uncertainty as to whether the smaller expansions in our samples reflect actual synapses, they were not examined in the present study. Qualitative observations confirmed the efficacy of distinguishing giant mossy fiber boutons from *en passant* terminals (or artifacts) based on size. Expansions greater than 4 μm^2 consistently exhibited the morphological characteristics of giant mossy fiber boutons, including irregular perimeters and the frequent presence of filopodia. In contrast, expansions less than 4 μm^2 typically had regular perimeters, were always "in line" with the main axon (giant boutons were sometimes connected to the main axon by short stalks), and never exhibited filopodia. Finally, filopodial extensions of giant mossy fiber boutons were also quantified. Similar to *en passant* terminals, filopodia also contact inhibitory interneurons; however, these synapses can be reliably identified by light microscopy (Acsády et al., 1998). Filopodial extensions were defined as protrusions exceeding 1 μm in length (Amaral, 1979; Amaral and Dent, 1981). At least 10 mossy fiber boutons from each animal were imaged for bouton and filopodial measurements. In addition, to determine mossy fiber bouton density, ~500–1,000 μm of mossy fiber axon per animal (5–6 separate axons) was imaged within CA3b.

Primary Dendrite Number

Primary dendrite number, defined as the number of dendrites originating from the soma of a neuron, was determined from up to nine adjacent sections from each animal using fluorescence microscopy. Sections were examined in series, and primary dendrite number was determined on every dentate granule cell meeting the selection criteria until 9–15

NIH-PA Author Manuscript

NIH-PA Author Manuscript

NIH-PA Author Manuscript

neurons were counted. To meet selection criteria the cell body had to be located on the dentate granule cell layer-molecular layer border or on the granule cell layer-hilar border (these populations were examined separately). The cell bodies of all neurons examined were contained within the tissue section, such that all primary dendrites could be accurately counted.

Spine Measurements

Images of granule cell dendrites were obtained from the inner, middle, and outer molecular layers. Regions were selected using fluorescent microscopy, and then imaged with the confocal microscope using a 63X (NA 1.4) objective at 6X optical zoom (approximate field size 40 μm). For each animal and region, dendrites from three different neurons were imaged. Figure 2 shows examples of regions selected for imaging inner (box 1), middle (box 2), and outer (box 3) molecular layer dendrites. Images were used to determine mean spine density and cross sectional profile area. For spine density, all spines along the selected dendritic segment were counted, and for profile area, every 10th spine was measured using Neurolucida software. Since spines begin to approach the limits of resolution of light microscopy, area measurements should be interpreted only relative to the other groups. Measurements of absolute spine areas would require electron microscopy. Importantly, however, light level area measurements avoid the arbitrary nature of classifying spines by type (mushroom, filopodial, etc.), since serial electron microscopy studies indicate a continuum of spine geometries in granule cells rather than distinct subclasses (Trommald and Hulleberg, 1997).

Statistics

For all statistical analyses, repeated measurements of a parameter from a single animal were averaged to avoid pseudoreplication. Statistical equivalence among $TrkB^{+/+}$ groups (synapsin cre positive $TrkB^{wt/wt}[+/+]$, synapsin cre negative $TrkB^{wt/wt}[+/+]$ and synapsin cre negative $TrkB^{flox/flox}[+/+]$) was assessed by analysis of variance (ANOVA). Equivalent groups were combined and compared to $TrkB^{-/-}$ mice using Student's *t*-test.

Figure Preparation

Confocal images are two-dimensional maximum projections generated from series of confocal images through the *z*-axis of the observed structure. Maximum projections were generated using Leica LCS software (version 2.61). Figures were prepared in Adobe Photoshop (version 7.0). In some cases, images are montages generated from the confocal z-series of a structure. This processing removed adjacent structures located above or below the observed structure which would obscure the two-dimensional representation. In no cases, however, was the neuronal structure that is the focus of a figure altered. Contrast and brightness were adjusted to optimize figure clarity. All images meant for comparison received identical adjustments. All images are pseudocolor.

RESULTS

GFP-Expressing Conditional $TrkB^{-/-}$ Mice

To assess the integrity of hippocampal dentate granule cell circuitry, conditional $TrkB^{-/-}$ mice were crossed to mice expressing GFP in a subset of dentate granule cells. In granule cells expressing GFP in this mouse line, GFP is readily detectable in dendrites (Fig. 3), dendritic spines (Fig. 7), mossy fiber axons (Fig. 5), and mossy fiber axon presynaptic terminals (Fig. 4). GFP-labeled granule cells in $TrkB^{-/-}$ mice appeared grossly normal, their structure being consistent with that described in previous studies (Cajal, 1911; Seress and Pokorny, 1981; Claiborne et al., 1986; Claiborne et al., 1990; Yan et al., 2001; Jones et al.,

NIH-PA Author Manuscript

NIH-PA Author Manuscript

NIH-PA Author Manuscript

2003). Granule cell dendrites projected into the molecular layer and terminated at the hippocampal fissure, while mossy fiber axons projected into the hilus and stratum lucidum. No qualitative disruptions in the laminar distribution of mossy fibers were noted relative to controls. The majority of mossy fibers were located in the hilus and stratum lucidum, with occasional fibers entering the pyramidal cell layer or infra-pyramidal region in CA3c. Within stratum lucidum, occasional GFP-labeled CA3 pyramidal cells were observed to possess thorny excrescences (not shown), the postsynaptic structures contacted by granule cell giant mossy fiber boutons. Although not quantified in the present study, the presence of these post-synaptic structures implies that TrkB is not required for their persistence.

Dentate Granule Cell Death Is Not Increased in TrkB$^{-/-}$ Mice

Among the hundreds of neurons examined in these animals, no GFP-labeled granule cells with obvious degenerative changes were observed. Consistent with this observation, staining with the degenerative cell marker Fluoro-Jade B revealed no qualitative increase in granule cell death (Fig. 1). Only two Fluoro-Jade B positive cells were found in the dentate in these animals; one from a TrkB$^{+/+}$ and one from a TrkB$^{-/-}$ mouse (not shown). These results suggest that TrkB is not required for the survival of the majority of granule cells, at least for the time point (two months) examined.

Granule Cells of TrkB $^{-/-}$ Mice Exhibit Increased Numbers of Filopodial Axonal Terminal Specializations

Filopodial extensions originate from granule cell mossy fiber boutons. To determine whether the number or structure of these extensions was altered in TrkB$^{-/-}$ mice, confocal microscopy was used to image 176 giant mossy fiber boutons and their associated filopodial extensions (112 boutons from 11 TrkB$^{+/+}$ mice and 64 boutons from 6 TrkB$^{-/-}$ mice). For each animal, at least 10 randomly selected giant boutons were imaged. Average filopodial length and number per mossy fiber bouton was determined from these images. In TrkB$^{-/-}$ mice, the number of filopodia per mossy fiber bouton was increased almost two-fold relative to TrkB$^{+/+}$ littermates (Fig. 4, TrkB$^{+/+}$, 0.77 ± 0.12; TrkB$^{-/-}$, 1.56 ± 0.25; $P < 0.01$). Average filopodial length, however, was not significantly altered (TrkB$^{+/+}$, 2.37 ± 0.24 μm; TrkB$^{-/-}$, 2.72 ± 0.31; $P = 0.39$). Filopodial extensions constitute part of an important feedforward inhibitory pathway that limits CA3 pyramidal cell excitation (Frotscher, 1989; Acsády et al., 1998; Seress et al., 2001). The present finding suggests that this inhibitory pathway is enhanced in TrkB$^{-/-}$ mice.

Mossy Fiber Bouton Density and Area Are Unchanged in TrkB$^{-/-}$ Mice

To determine whether granule cell-CA3 pyramid contacts might also be altered in TrkB$^{-/-}$ mice, the structure and density of giant mossy fiber boutons was determined using confocal microscopy and quantitative neuronal reconstructions. Giant boutons were present and appeared grossly normal in the TrkB$^{-/-}$ mice. Giant boutons can contain more than 30 synaptic release sites and are packed with synaptic vesicles (Chicurel and Harris, 1992; Acsády et al., 1998). Changes in the number of release sites and/or synaptic vesicle content might be reflected by changes in bouton size (Pierce and Milner, 2001). An analysis of the cross sectional area of individual boutons, however, revealed no significant differences between TrkB$^{-/-}$ and TrkB$^{+/+}$ mice (Fig. 4; TrkB$^{+/+}$, 10.60 ± 0.35 μm^2; TrkB$^{-/-}$, 10.62 ± 0.52 μm^2). Moreover, no difference in the number of mossy fiber boutons per 100 μm of axon was found between TrkB$^{-/-}$ and TrkB$^{+/+}$ mice (Fig. 5; TrkB$^{+/+}$, 0.96 ± 0.05 MFB/100 μm; TrkB$^{-/-}$, 1.06 ± 0.08).

NIH-PA Author Manuscript

NIH-PA Author Manuscript

NIH-PA Author Manuscript

Soma Area Is Unaffected by TrkB Deletion

Mean soma profile area was determined from 144 granule cells from $TrkB^{+/+}$ mice and 72 granule cells from $TrkB^{-/-}$ mice. Mean profile area was unchanged in $TrkB^{-/-}$ mice relative to wildtype littermates ($TrkB^{+/+}$, 91.0 ± 2.3 μm^2; $TrkB^{-/-}$, 90.6 ± 6.2; $P = 0.931$).

Decreased Dendrite Number in $TrkB^{-/-}$ Mice

In addition to regulating synaptic terminal properties, TrkB is implicated in regulating the formation of new dendrites. Specifically, overexpression of the TrkB ligand BDNF increased dendrite number both in vitro (Danzer et al., 2002) and in vivo (Tolwani et al., 2002). To determine whether dendrite formation was reduced in $TrkB^{-/-}$ mice, primary dendrite number was determined for two populations of granule cells; those located along the granule cell-molecular layer border and those located along the granule cell layer-hilar border. These two populations are morphologically distinct, with the former typically possessing multiple primary dendrites and the latter typically only a single, radially projecting dendrite (Cajal, 1911; Green and Juraska, 1985; Claiborne et al., 1990; Ambrogini et al., 2004; Redila and Christie, 2006). Along the molecular layer border, 111 granule cells from 11 $TrkB^{+/+}$ mice and 57 granule cells from 6 $TrkB^{-/-}$ animals were examined. A 27% reduction in number of primary dendrites was detected among granule cells of $TrkB^{-/-}$ mice relative to $TrkB^{+/+}$ littermates (Fig. 6; $TrkB^{+/+}$, 2.79 ± 0.09; $TrkB^{-/-}$, 2.03 ± 0.15; $P < 0.001$). In contrast, examination of 196 granule cells located along the hilar border (114 cells from 11 $TrkB^{+/+}$ mice, 82 from 6 $TrkB^{-/-}$ mice) revealed no difference in primary dendrite number (Fig. 3). As expected, the majority of these cells exhibited only a single primary dendrite ($TrkB^{+/+}$, 1.08 ± 0.03; $TrkB^{-/-}$, 1.08 ± 0.05; $P = 0.944$). These findings suggest that endogenous TrkB may play a role in promoting the formation of additional primary dendrites for older granule cells located along the molecular layer border.

Increased Spine Area in $TrkB^{-/-}$ Mice

To determine whether granule cells exhibiting reduced dendrite number also exhibited changes in spine number or structure, the proximal dendrites of granule cells located along the molecular layer border were imaged using confocal microscopy. Excitatory synaptic inputs to the inner third of the granule cell dendritic tree are derived principally from associational-commissural afferents. Here, dendritic spines in the inner molecular layer receiving these inputs were examined. For each animal, three dendritic segments from three different neurons were examined (33 segments from 11 $TrkB^{+/+}$ mice, 18 segments from 6 $TrkB^{-/-}$ mice).

Spine density was not significantly altered in the inner molecular layer of $TrkB^{-/-}$ mice relative to littermate controls ($TrkB^{+/+}$, 1.51 ± 0.08 spines/μm; $TrkB^{-/-}$, 1.45 ± 0.12), suggesting similar numbers of associational-commissural inputs between genotypes. A statistical power analysis of these data revealed a 99% chance of detecting a 50% change in spine density. Any undetected changes in spine density, if existent, are therefore likely smaller than this. Casual observation of inner molecular layer dendrites, however, revealed numerous enlarged spines in $TrkB^{-/-}$ mice relative to littermate controls. To quantify this effect, the profile area of every 10th spine was measured from the confocal images used for spine counts, producing a sample of 25–30 spines per animal. This analysis revealed a significant increase in mean spine profile area in $TrkB^{-/-}$ mice relative to controls (Fig. 7). In controls, mean spine area was 0.27 ± 0.01 μm^2, whereas in $TrkB^{-/-}$ mice area was increased to 0.33 ± 0.02 μm^2 ($P < 0.01$). These findings suggest altered postsynaptic terminal function in $TrkB^{-/-}$ mice.

Finally, spine density and area were examined along the outer and middle thirds of the granule cell dendritic tree; although in this case for technical reasons granule cells for

NIH-PA Author Manuscript

NIH-PA Author Manuscript

NIH-PA Author Manuscript

analysis were selected from throughout the superior blade of the DG, rather than just those cells with their somas located along the molecular layer border. For each animal, three dendritic segments from three different neurons were examined (33 segments from 11 $TrkB^{+/+}$ mice, 18 segments from 6 $TrkB^{-/-}$ mice). As in the inner molecular layer, spine density was not altered in the middle or outer molecular layers ($TrkB^{+/+}$: middle, 2.79 ± 0.18 spines/μm^2; outer, 2.16 ± 0.14; $TrkB^{-/-}$: middle, 2.44 ± 0.22; outer, 2.15 ± 0.20). Statistical power in these analyses was 99% for detecting a 50% change. Spine profile area was increased in the outer third; however, with a mean of 0.30 ± 0.02 μm^2 in $TrkB^{+/+}$ mice and 0.37 ± 0.02 μm^2 in $TrkB^{-/-}$ mice (Fig. 7, *t*-test, $P = 0.039$). Mean spine area in the middle molecular layer was not significantly altered in $TrkB^{-/-}$ mice relative to littermate controls ($TrkB^{+/+}$, 0.24 ± 0.01; $TrkB^{-/-}$, 0.25 ± 0.02, *t*-test, $P = 0.576$).

DISCUSSION

Here we examined the role of TrkB in regulating the synaptic structures of hippocampal dentate granule cells. Both post-synaptic and presynaptic structures were assessed to gain insight into whether TrkB modifies the morphological substrates of granule cell connectivity. Both were altered. Postsynaptically, granule cells exhibited fewer primary dendrites whereas dendritic spines on these dendrites were larger in area in $TrkB^{-/-}$ mice relative to wildtype littermates. Presynaptically, conditional deletion of TrkB increased the number of filopodia per giant mossy fiber bouton. In contrast, the size and density of giant mossy fiber boutons was unchanged. Together, these findings suggest altered cortical and associational/commissural input to dentate granule cells and enhanced feedforward inhibition of CA3 pyramidal cells.

The present study relies on anatomical methods to assess presynaptic and postsynaptic terminals in $TrkB^{-/-}$ mice and littermate controls. Changes in the number and/or structure of spines and boutons guide predictions as to the functional consequences of TrkB elimination. Physiological studies, however, are ultimately required to test these predictions. Importantly, it is unclear whether the changes identified in the $TrkB^{-/-}$ mice are triggered by the absence of TrkB within granule cells themselves or from afferents or targets of the granule cells or from synaptically remote locales. Likewise, it is unclear whether the changes found are an immediate consequence of the absence of TrkB or due to some homeostatic response to the absence of TrkB. With these caveats in mind, the present results do provide clear insights into the impact of TrkB on granule cell connectivity.

TrkB does not appear to be required for granule cell survival or gross morphological stability. Degeneration of cortical neurons has been reported following conditional deletion of TrkB (Xu et al., 2000). Granule cells, on the other hand, appeared surprising normal after the elimination of TrkB. Previous analyses of Nissl-stained sections likewise revealed no overt abnormalities or obvious loss of granule cells (He et al., 2004). Similarly, in the present study degenerating GFP-labeled granule cells were not observed, and no increase in Fluoro-Jade B labeling of dying granule cells was apparent in two-month-old animals. Importantly, in the Thy-GFP expressing mouse line studied here, dentate granule cells do not begin to express GFP until they are about four-weeks-old (Walter et al., 2007), the obvious implication being that the cells examined in the present study survived for at least this long. We did not conduct stereological cell counts, so we cannot exclude the possibility of more subtle differences in cell numbers (Lähteinen et al., 2003), nor can we rule out the possibility that death increases in older animals (von Bohlen und Halbach et al., 2003; Baquet et al., 2004). The majority of granule cells, however, appear to survive into adulthood. Similarly, granule cell polarity was not disrupted in these animals. Dendrites were found to project from the top of the soma into the molecular layer, and granule cell mossy fiber axons projected into the hilus. The area, density, and spatial distribution of giant

NIH-PA Author Manuscript

NIH-PA Author Manuscript

NIH-PA Author Manuscript

mossy fiber boutons were also not altered in $TrkB^{-/-}$ mice. The present results contrast with prior analyses of CNS histology and mossy fiber terminals in conventional TrkB knockout mice. With conventional knockouts, TrkB is eliminated from every cell in the animal for the entire lifespan. In contrast, the conditional strategy used here temporally and spatially restricts the elimination of TrkB to CNS neurons following expression of synapsin I-driven Cre recombinase. Conventional elimination of TrkB results in numerous nervous system lesions and neonatal death within two to three weeks (Alcántara et al., 1997). Early death is likely a consequence of myocardial pathology in these animals (Donovan et al., 2000). At a subcellular level, 11 to 12-day-old conventional TrkB knockout mice exhibit reduced numbers of mossy fiber boutons, with remaining boutons being smaller in size and possessing fewer synaptic terminals (Otal et al., 2005). Whether the earlier elimination, broader tissue distribution, broader cellular distribution, and/or the poor health of conventional TrkB knockouts account for differences between the current and prior studies is not clear. That said, our findings suggest that granule cell survival and the persistence of gross structural characteristics does not require TrkB.

Although gross disruption of granule cell structure was not observed, granule cells from $TrkB^{-/-}$ mice did exhibit fewer primary dendrites relative to cells from control mice. This finding is consistent with previous studies in which BDNF overexpression, both in vivo (Tolwani et al., 2002) and in vitro (Danzer et al., 2002), led to an increase in primary dendrite number among granule cells. Together, these studies support the idea that TrkB activation promotes primary dendrite formation of the granule cells. Interestingly, only granule cells located along the molecular layer border exhibited decreases. Primary dendrite number for granule cells located along the hilar border was equivalent between genotypes. Granule cells located on the molecular border are in general older than cells on the hilar border (Altman and Das, 1965; Altman and Bayer, 1990), and typically possess more primary dendrites than their younger neighbors (which usually have only a single primary dendrite). Together this suggests that activation of TrkB during the maturation of granule cells contributes to formation of its dendritic arbor. Finally, the functional consequences of increased or decreased numbers of primary dendrites are not clear. Changes in primary dendrite number could reflect changes in total dendritic length or a redistribution of dendritic structures. Either scenario might result in dramatic changes in the number and/or type of synaptic inputs received by a cell. Similarly, changes in dendritic structure would also alter passive electrotonic properties. Changes in EPSP summation or transmission to the axon hillock would be likely consequences.

Further evidence for a role of TrkB in regulating granule cell synaptic inputs comes from analysis of dendritic spines. Although spine density was unchanged in $TrkB^{-/-}$ mice, spine area was significantly increased along dendritic segments in the inner and outer molecular layers. These findings are consistent with recent studies examining $TrkB^{flox/flox}$CaMKII-CRE mice, in which granule cell spine density was not altered, but mean spine length was significantly increased (von Bohlen und Halbach et al., 2006). Interestingly, changes in granule cell spine structure may result from alterations in entorhinal and associational/commissural inputs (Frotscher et al., 2000). These inputs exhibited reduced numbers of collaterals and varicosities in conventional $TrkB^{-/-}$ mice (Martinez et al., 1998). Alternatively, the absence of TrkB within the spine itself may result in reduced spine area, perhaps via reduced calcium entry through the transient receptor potential channel (TRPC) family of ion channels (Tyler and Pozzo-Miller, 2003; Pozzo-Miller, 2006; Amaral and Pozzo-Miller, 2007). Finally, whether increased spine area reflects reduced synaptic function, (Gonzalez et al., 1999; Kovalchuk et al., 2002; Elmariah et al., 2004) remains to be determined.

NIH-PA Author Manuscript

NIH-PA Author Manuscript

NIH-PA Author Manuscript

The present data suggest that elimination of TrkB altered the number of granule cell-inhibitory interneuron synapses but not granule cell-CA3 pyramidal cell synapses. In $TrkB^{-/-}$ mice, the number of filopodial extensions per mossy fiber bouton was significantly increased. These filopodia make synaptic contact with inhibitory interneurons, which in turn provide feedforward inhibition to CA3 pyramidal cells. Increased numbers of filopodia suggest a strengthening of this inhibitory pathway. In contrast, neither the size nor density of granule cell-CA3 pyramidal cell synapses were altered in $TrkB^{-/-}$ mice. Whether other parameters of this synapse are modulated by TrkB deletion is not known. Our findings are consistent; however, with recent physiological studies indicating normal basal synaptic activation of CA3 pyramidal cells by mossy fibers in slices from $TrkB^{-/-}$ mice (Huang et al., in press). These results are also consistent with work by De Paola et al. (2003), in which they demonstrated in vitro that BDNF treatment led to rapid changes in filopodia dynamics, while giant boutons were comparatively stable. Interestingly, a number of studies now demonstrate a role for TrkB in regulating GABAergic synaptic transmission (Bolton et al., 2000; Carmona et al., 2003; Carmona et al., 2006; Singh et al., 2006; Swanwick et al., 2006; Kohara et al., 2007). The present study extends these findings by demonstrating that TrkB can also act upstream of the GABAergic neuron, regulating excitatory input to these cells. Conditional deletion of the TrkB gene leads to a striking impairment of epileptogenesis in the kindling model of epilepsy (He at al., 2004). A disproportionate increase in the strength of feedforward inhibition compared to excitation of CA3 pyramidal cells by mossy fiber axons of $TrkB^{-/-}$ mice may contribute to this impairment.

Acknowledgments

Grant sponsor: NIH; Grant number: R01-NS-056217; Grant sponsors: NIH, Epilepsy Foundation, the Ruth K. Broad Foundation, Cincinnati Children's Hospital Research Foundation.

$TrkB^{flox/flox}$ mice were provided by Dr. Luis Parada (UT Southwestern) and Thy1-GFP mice by Dr. Guoping Feng (Duke University). We would also like to thank Keri Kaeding and Lauren King for useful comments on earlier versions of this manuscript.

References

Acsády L, Kamondi A, Sik A, Freund T, Buzsaki G. GABAergic cells are the major postsynaptic targets of mossy fibers in the rat hippocampus. J Neurosci. 1998; 18:3386–3403. [PubMed: 9547246]

Alcántara S, Frisen J, del Rio JA, Soriano E, Barbacid M, Silos-Santiago I. TrkB signaling is required for postnatal survival of CNS neurons and protects hippocampal and motor neurons from axotomy-induced cell death. J Neurosci. 1997; 15:3623–3633.

Altman J, Das GD. Autoradiographic and histological evidence of postnatal hippocampal neurogenesis in rats. J Comp Neurol. 1965; 124:319–335. [PubMed: 5861717]

Altman J, Bayer SA. Migration and distribution of two populations of hippocampal granule cell precursors during the perinatal and postnatal periods. J Comp Neurol. 1990; 301:365–381. [PubMed: 2262596]

Amaral DG. Synaptic extensions from the mossy fibers of the fascia dentata. Anat Embryol (Berl). 1979; 155:241–251. [PubMed: 453543]

Amaral DG, Dent JA. Development of the mossy fibers of the dentate gyrus. I. A light and electron microscopic study of the mossy fibers and their expansions. J Comp Neurol. 1981; 195:51–86. [PubMed: 7204652]

Amaral MD, Pozzo-Miller L. TRPC3 channels are necessary for brain-derived neurotrophic factor to activate a nonselective cationic current and to induce dendritic spine formation. J Neurosci. 2007; 27:5179–5189. [PubMed: 17494704]

Ambrogini P, Lattanzi D, Ciuffoli S, Agostini D, Bertini L, Stocchi V, Santi S, Cuppini R. Morpho-functional characterization of neuronal cells at different stages of maturation in granule cell layer of adult rat dentate gyrus. Brain Res. 2004; 1017(1/2):21–31. [PubMed: 15261095]

NIH-PA Author Manuscript

NIH-PA Author Manuscript

NIH-PA Author Manuscript

Asztely F, Kokaia M, Olofsdotter K, Ortegren U, Lindvall O. Afferent-specific modulation of short-term synaptic plasticity by neurotrophins in dentate gyrus. Eur J Neurosci. 2000; 12:662–669. [PubMed: 10712646]

Baquet ZC, Gorski JA, Jones KR. Early striatal dendrite deficits followed by neuron loss with advanced age in the absence of anterograde cortical brain-derived neurotrophic factor. J Neurosci. 2004; 24:4250–4258. [PubMed: 15115821]

Binder DK, Routbort MJ, McNamara JO. Immunohistochemical evidence of seizure-induced activation of trk receptors in the mossy fiber pathway of adult rat hippocampus. J Neurosci. 1999; 19:4616–4626. [PubMed: 10341259]

Binder DK, Scharfman HE. Brain-derived neurotrophic factor. Growth Factors. 2004; 22:123–131. [PubMed: 15518235]

Bolton M, Pittman AJ, Lo DC. Brain-derived neurotrophic factor differentially regulates excitatory and inhibitory synaptic transmission in hippocampal cultures. J Neurosci. 2000; 20:3221–3232. [PubMed: 10777787]

Bramham CR, Messaoudi E. BDNF function in adult synaptic plasticity: The synaptic consolidation hypothesis. Prog Neurobiol. 2005; 76:99–125. [PubMed: 16099088]

Cajal, SR. The Structure of Ammon's Horn. Springfield, IL: Charles C. Thomas; 1911.

Carmona MA, Martinez A, Soler A, Blasi J, Soriano E, Aguado F. Ca(2+)-evoked synaptic transmission and neurotransmitter receptor levels are impaired in the forebrain of trkb (−/−) mice. Mol Cell Neurosci. 2003; 22:210–226. [PubMed: 12676531]

Carmona MA, Pozas E, Martinez A, Espinosa-Parrilla JF, Soriano E, Aguado F. Age-dependent spontaneous hyperexcitability and impairment of GABAergic function in the hippocampus of mice lacking trkB. Cereb Cortex. 2006; 16:47–63. [PubMed: 15829735]

Chicurel ME, Harris KM. Three-dimensional analysis of the structure and composition of CA3 branched dendritic spines and their synaptic relationships with mossy fiber boutons in the rat hippocampus. J Comp Neurol. 1992; 325:169–182. [PubMed: 1460112]

Claiborne BJ, Amaral DG, Cowan WM. A light and electron microscopic analysis of the mossy fibers of the rat dentate gyrus. J Comp Neurol. 1986; 246:435–458. [PubMed: 3700723]

Claiborne BJ, Amaral DG, Cowan WM. Quantitative, three-dimensional analysis of granule cell dendrites in the rat dentate gyrus. J Comp Neurol. 1990; 302:206–219. [PubMed: 2289972]

Conner JM, Lauterborn JC, Yan Q, Gall CM, Varon S. Distribution of brain-derived neurotrophic factor (BDNF) protein and mRNA in the normal adult rat CNS: evidence for anterograde axonal transport. J Neurosci. 1997; 17:2295–2313. [PubMed: 9065491]

Croll SD, Suri C, Compton DL, Simmons MV, Yancopoulos GD, Lindsay RM, Wiegand SJ, Rudge JS, Scharfman HE. Brain-derived neurotrophic factor transgenic mice exhibit passive avoidance deficits, increased seizure severity and in vitro hyperexcitability in the hippocampus and entorhinal cortex. Neuroscience. 1999; 93:1491–1506. [PubMed: 10501474]

Danzer SC, Crooks KR, Lo DC, McNamara JO. Increased expression of brain-derived neurotrophic factor induces formation of basal dendrites and axonal branching in dentate granule cells in hippocampal explant cultures. J Neurosci. 2002; 22:9754–9763. [PubMed: 12427830]

Danzer SC, Pan E, Nef S, Parada LF, McNamara JO. Altered Regulation of BDNF Protein in Hippocampus Following Slice Preparation. Neuroscience. 2004a; 126:859–869. [PubMed: 15207321]

Danzer SC, He XP, McNamara JO. Ontogeny of Seizure-induced increases in BDNF Immunoreactivity and TrkB receptor activation in rat hippocampus. Hippocampus. 2004b; 14:345–355. [PubMed: 15132434]

Danzer SC, McNamara JO. Localization of BDNF to distinct terminals of mossy fiber axons implies regulation of both excitation and feedforward inhibition of CA3 pyramidal cells. J Neurosci. 2004; 24:11346–11355. [PubMed: 15601941]

Desmond NL, Levy WB. Granule cell dendritic spine density in the rat hippocampus varies with spine shape and location. Neurosci Lett. 1985; 54(2/3):219–224. [PubMed: 3991060]

De Paola V, Arber S, Caroni P. AMPA receptors regulate dynamic equilibrium of presynaptic terminals in mature hippocampal networks. Nat Neurosci. 2003; 6:491–500. [PubMed: 12692557]

NIH-PA Author Manuscript

NIH-PA Author Manuscript

NIH-PA Author Manuscript

Donovan MJ, Lin MI, Wiegn P, Ringstedt T, Kraemer R, Hahn R, Wang S, Ibanez CF, Rafii S, Hempstead BL. Brain derived neurotrophic factor is an endothelial cell survival factor required for intramyocardial vessel stabilization. Development. 2000; 127:4531–4540. [PubMed: 11023857]

Elmariah SB, Crumling MA, Parsons TD, Balice-Gordon RJ. Postsynaptic TrkB-mediated signaling modulates excitatory and inhibitory neurotransmitter receptor clustering at hippocampal synapses. J Neurosci. 2004; 24:2380–2393. [PubMed: 15014113]

Feng G, Mellor RH, Bernstein M, Keller-Peck C, Nguyen QT, Wallace M, Nerbonne JM, Lichtman JW, Sanes JR. Imaging neuronal subsets in transgenic mice expressing multiple spectral variants of GFP. Neuron. 2000; 28:41–51. [PubMed: 11086982]

Frotscher M. Mossy fiber synapses on glutamate decarboxylase-immunoreactive neurons: Evidence for feed-forward inhibition in the CA3 region of the hippocampus. Exp Brain Res. 1989; 75:441–445. [PubMed: 2721621]

Frotscher M, Drakew A, Heimrich B. Role of afferent innervation and neuronal activity in dendritic development and spine maturation of fascia dentata granule cells. Cereb Cortex. 2000; 10:946–951. [PubMed: 11007545]

Gonzalez M, Ruggiero FP, Chang Q, Shi YJ, Rich MM, Kraner S, Balice-Gordon RJ. Disruption of Trkb-mediated signaling induces disassembly of postsynaptic receptor clusters at neuromuscular junctions. Neuron. 1999; 24:567–583. [PubMed: 10595510]

Green EJ, Juraska JM. The dendritic morphology of hippocampal dentate granule cells varies with their position in the granule cell layer: A quantitative Golgi study. Exp Brain Res. 1985; 59:582–586. [PubMed: 2411588]

Gu H, Marth JD, Orban PC, Mossmann H, Rajewsky K. Deletion of a DNA polymerase beta gene segment in T cells using cell type-specific gene targeting. Science. 1994; 265:103–106. [PubMed: 8016642]

Huang YZ, Pan E, Xiong Z-Q, McNamara JO. Zinc-mediated trans-activation of TrkB Potentiates the hippocampal mossy fiber-CA3 pyramid synapse. Neuron. (in press).

He XP, Minichiello L, Klein R, McNamara JO. Immunohistochemical evidence of seizure-induced activation of trkB receptors in the mossy fiber pathway of adult mouse hippocampus. J Neurosci. 2002; 22:7502–7508. [PubMed: 12196573]

He XP, Kotloski R, Nef S, Luikart BW, Parada LF, McNamara JO. Conditional deletion of TrkB but not BDNF prevents epileptogenesis in the kindling model. Neuron. 2004; 43:31–42. [PubMed: 15233915]

Henze DA, Wittner L, Buzsaki G. Single granule cells reliably discharge targets in the hippocampal CA3 network in vivo. Nat Neurosci. 2002; 5:790–795. [PubMed: 12118256]

Ishizuka N, Cowan WM, Amaral DG. A quantitative analysis of the dendritic organization of pyramidal cells in the rat hippocampus. J Comp Neurol. 1995; 362:17–45. [PubMed: 8576427]

Jones SP, Rahimi O, O'Boyle MP, Diaz DL, Claiborne BJ. Maturation of granule cell dendrites after mossy fiber arrival in hippocampal field CA3. Hippocampus. 2003; 13:413–427. [PubMed: 12722981]

Kokaia M, Ernfors P, Kokaia Z, Elmér E, Jaenisch R, Lindvall O. Suppressed epileptogenesis in BDNF mutant mice. Exp Neurol. 1995; 133:215–224. [PubMed: 7649227]

Kovalchuk Y, Hanse E, Kafitz KW, Konnerth A. Postsynaptic induction of BDNF-mediated long-term potentiation. Science. 2002; 295:1729–1734. [PubMed: 11872844]

Kohara K, Yasuda H, Huang Y, Adachi N, Sohya K, Tsumoto T. A local reduction in cortical GABAergic synapses after a loss of endogenous brain-derived neurotrophic factor, as revealed by single-cell gene knock-out method. J Neurosci. 2007; 27:7234–7244. [PubMed: 17611276]

Lähteinen S, Pitkänen A, Saarelainen T, Nissinen J, Koponen E, Castrén E. Decreased BDNF signaling in transgenic mice reduces epileptogenesis. Eur J Neurosci. 2002; 15:721–734. [PubMed: 11886452]

Lähteinen S, Pitkänen A, Koponen E, Saarelainen T, Castrén E. Exacerbated status epilepticus and acute cell loss, but no changes in epileptogenesis, in mice with increased brain-derived neurotrophic factor signaling. Neuroscience. 2003; 122:1081–1092. [PubMed: 14643774]

Lorente de Nó R. Studies on the structure of the cerebral cortex. II. Continuation of the study of the ammonic system. J Psychol Neurol (Lpz). 1934; 46:113–177.

NIH-PA Author Manuscript

NIH-PA Author Manuscript

NIH-PA Author Manuscript

Mathern GW, Babb TL, Micevych PE, Blanco CE, Pretorius JK. Granule cell mRNA levels for BDNF, NGF, and NT-3 correlate with neuron losses or supragranular mossy fiber sprouting in the chronically damaged and epileptic human hippocampus. Mol Chem Neuropathol. 1997; 30(1/2): 53–76. [PubMed: 9138429]

Martinez A, Alcantara S, Borrell V, Del Rio JA, Blasi J, Otal R, Campos N, Boronat A, Barbacid M, Silos-Santiago I, Soriano E. TrkB and TrkC signaling are required for maturation and synaptogenesis of hippocampal connections. J Neurosci. 1998; 18:7336–7350. [PubMed: 9736654]

Messaoudi E, Bardsen K, Srebro B, Bramham CR. Acute intra-hippocampal infusion of BDNF induces lasting potentiation of synaptic transmission in the rat dentate gyrus. J Neurophysiol. 1998; 79:496–499. [PubMed: 9425220]

Murray KD, Isackson PJ, Eskin TA, King MA, Montesinos SP, Abraham LA, Roper SN. Altered mRNA expression for brain-derived neurotrophic factor and type II calcium/calmodulin-dependent protein kinase in the hippocampus of patients with intractable temporal lobe epilepsy. J Comp Neurol. 2000; 418:411–422. [PubMed: 10713570]

Olofsdotter K, Lindvall O, Asztely F. Increased synaptic inhibition in dentate gyrus of mice with reduced levels of endogenous brain-derived neurotrophic factor. Neuroscience. 2000; 101:531–539. [PubMed: 11113302]

Otal R, Martinez A, Soriano E. Lack of TrkB and TrkC signaling alters the synaptogenesis and maturation of mossy fiber terminals in the hippocampus. Cell Tissue Res. 2005; 319:349–358. [PubMed: 15726425]

Paxinos, G.; Franklin, KBJ. The Mouse Brain in Stereotaxic Coordinates. 2. New York: Academic Press; 2001.

Pierce JP, Milner TA. Parallel increases in the synaptic and surface areas of mossy fiber terminals following seizure induction. Synapse. 2001; 39:249–256. [PubMed: 11169773]

Pozzo-Miller L. BDNF enhances dendritic Ca^{2+} signals evoked by coincident EPSPs and back-propagating action potentials in CA1 pyramidal neurons. Brain Res. 2006; 1104:45–54. [PubMed: 16797499]

Redila VA, Christie BR. Exercise-induced changes in dendritic structure and complexity in the adult hippocampal dentate gyrus. Neuroscience. 2006; 137:1299–1307. [PubMed: 16338077]

Scharfman HE, Goodman JH, Sollas AL. Actions of brain-derived neurotrophic factor in slices from rats with spontaneous seizures and mossy fiber sprouting in the dentate gyrus. J Neurosci. 1999; 19:5619–5631. [PubMed: 10377368]

Schmued LC, Albertson C, Slikker W Jr. Fluoro-Jade: A novel fluorochrome for the sensitive and reliable histochemical localization of neuronal degeneration. Brain Res. 1997; 751:37–46. [PubMed: 9098566]

Seress L, Pokorny J. Structure of the granular layer of the rat dentate gyrus. A light microscopic and Golgi study. J Anat. 1981; 133 (Part 2):181–195. [PubMed: 7333948]

Seress L, Abrahám H, Paleszter M, Gallyas F. Granule cells are the main source of excitatory input to a subpopulation of GABAergic hippocampal neurons as revealed by electron microscopic double staining for zinc histochemistry and parvalbumin immunocytochemistry. Exp Brain Res. 2001; 136:456–462. [PubMed: 11291726]

Singh B, Henneberger C, Betances D, Arevalo MA, Rodriguez-Tebar A, Meier JC, Grantyn R. Altered balance of glutamatergic/GABAergic synaptic input and associated changes in dendrite morphology after BDNF expression in BDNF-deficient hippocampal neurons. J Neurosci. 2006; 26:7189–7200. [PubMed: 16822976]

Swanwick CC, Murthy NR, Kapur J. Activity-dependent scaling of GABAergic synapse strength is regulated by brain-derived neurotrophic factor. Mol Cell Neurosci. 2006; 31:481–492. [PubMed: 16330218]

Takahashi M, Hayashi S, Kakita A, Wakabayashi K, Fukuda M, Kameyama S, Tanaka R, Takahashi H, Nawa H. Patients with temporal lobe epilepsy show an increase in brain-derived neurotrophic factor protein and its correlation with neuropeptide Y. Brain Res. 1999; 818:579–582. [PubMed: 10082852]

NIH-PA Author Manuscript

NIH-PA Author Manuscript

NIH-PA Author Manuscript

Tolwani RJ, Buckmaster PS, Varma S, Cosgaya JM, Wu Y, Suri C, Shooter EM. BDNF overexpression increases dendrite complexity in hippocampal dentate gyrus. Neuroscience. 2002; 114:795–805. [PubMed: 12220579]

Trommald M, Hulleberg G. Dimensions and density of dendritic spines from rat dentate granule cells based on reconstructions from serial electron micrographs. J Comp Neurol. 1997; 377:15–28. [PubMed: 8986869]

Tyler WJ, Pozzo-Miller L. Miniature synaptic transmission and BDNF modulate dendritic spine growth and form in rat CA1 neurones. J Physiol. 2003; 553(Part 2):497–509. [PubMed: 14500767]

von Bohlen und Halbach O, Minichiello L, Unsicker K. Haploinsufficiency in trkB and/or trkC neurotrophin receptors causes structural alterations in the aged hippocampus and amygdala. Eur J Neurosci. 2003; 18:2319–2325. [PubMed: 14622193]

von Bohlen und Halbach O, Krause S, Medina D, Sciarretta C, Minichiello L, Unsicker K. Regional- and age-dependent reduction in trkB receptor expression in the hippocampus is associated with altered spine morphologies. Biol Psychiatry. 2006; 59:793–800. [PubMed: 16325153]

Walter C, Murphy BL, Pun RY, Spieles-Engemann AL, Danzer SC. Pilocarpine-induced seizures cause selective time-dependent changes to adult-generated hippocampal dentate granule cells. J Neurosci. 2007; 27:7541–7552. [PubMed: 17626215]

Xu B, Zang K, Ruff NL, Zhang YA, McConnell SK, Stryker MP, Reichardt LF. Cortical degeneration in the absence of neurotrophin signaling: Dendritic retraction and neuronal loss after removal of the receptor TrkB. Neuron. 2000; 26:233–245. [PubMed: 10798407]

Yan XX, Spigelman I, Tran PH, Ribak CE. Atypical features of rat dentate granule cells: recurrent basal dendrites and apical axons. Anat Embryol (Berl). 2001; 203:203–209. [PubMed: 11303906]

Zhu Y, Romero MI, Ghosh P, Ye Z, Charnay P, Rushing EJ, Marth JD, Parada LF. Ablation of NF1 function in neurons induces abnormal development of cerebral cortex and reactive gliosis in the brain. Genes Dev. 2001; 15:859–876. [PubMed: 11297510]

Zhu WJ, Roper SN. Brain-derived neurotrophic factor enhances fast excitatory synaptic transmission in human epileptic dentate gyrus. Ann Neurol. 2001; 50:188–194. [PubMed: 11506401]

NIH-PA Author Manuscript
NIH-PA Author Manuscript
NIH-PA Author Manuscript

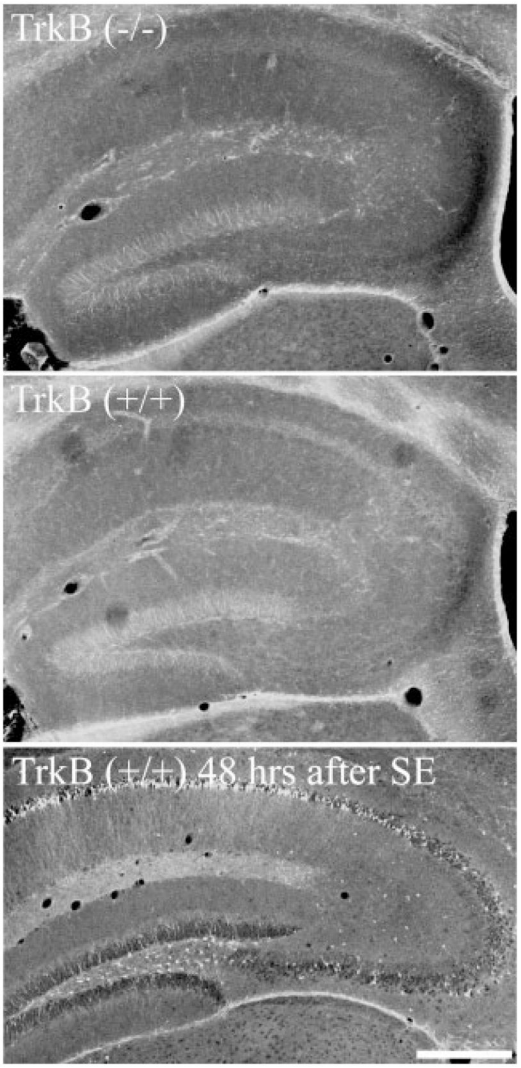

FIGURE 1.

Fluoro-Jade B labeling of $TrkB^{+/+}$ and $TrkB^{-/-}$ mice. Note the absence of labeled cells in both genotypes. Lower panel: Positive control section from an animal killed 48 h after pilocarpine-status epilepticus (SE) showing extensive Fluoro-Jade B staining (demonstrating neuronal loss) in the dentate hilus, CA1 and CA3. Scale bar = 375 μm.

NIH-PA Author Manuscript
NIH-PA Author Manuscript
NIH-PA Author Manuscript

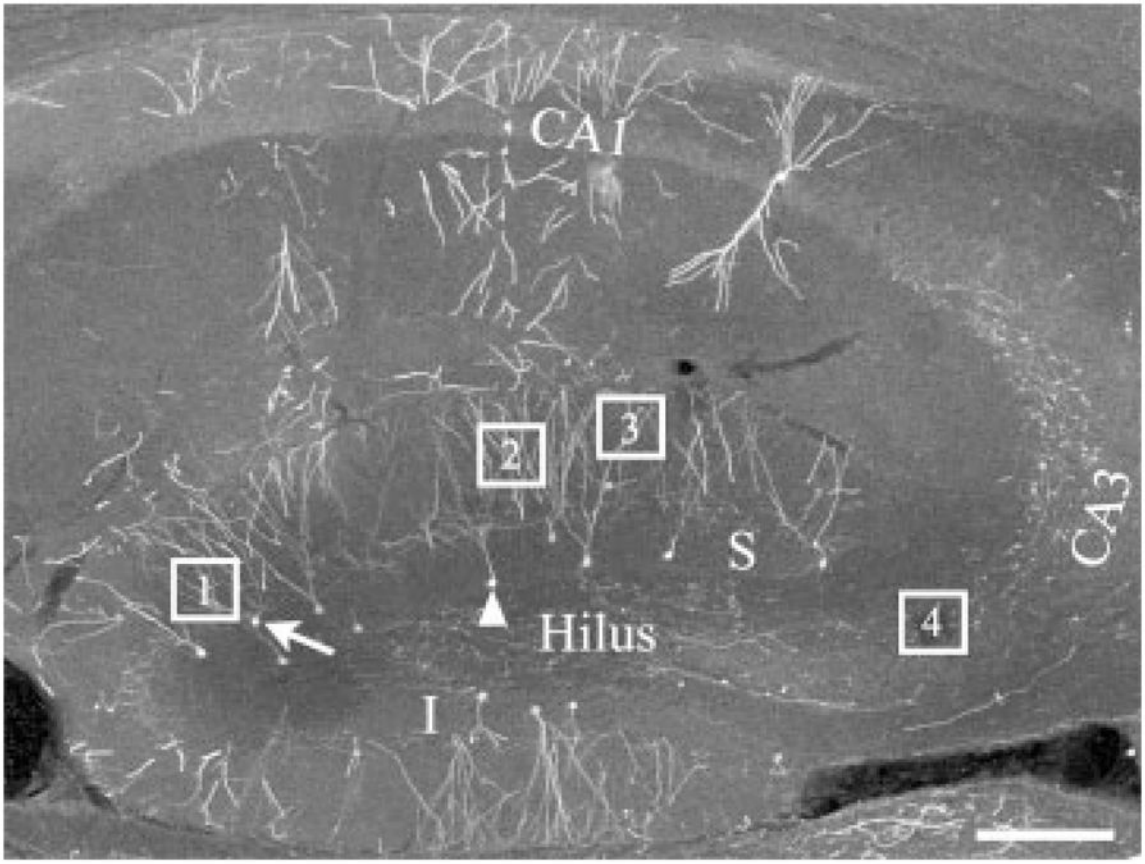

FIGURE 2.

Confocal image of the hippocampus of a GFP-expressing mouse showing the regions where measurements were taken from. S, superior blade of the DG; I, inferior blade of the DG; Box 1, example of an inner molecular layer granule cell dendrite; Box 2, example of a middle molecular layer granule cell dendrite; Box 3, example of an outer molecular layer granule cell dendrite; Box 4, sampling region used for examining mossy fiber boutons and filopodia; Arrow, example of a dentate granule cell on the molecular layer border for counting primary dendrite number, inner molecular layer spine area, and density. Arrowhead, example of a granule cell on the hilar border used for counting primary dendrite number; CA3, CA3 pyramidal cell layer; CA1, CA1 pyramidal cell layer. Scale bar = 150 μm.

NIH-PA Author Manuscript

NIH-PA Author Manuscript

NIH-PA Author Manuscript

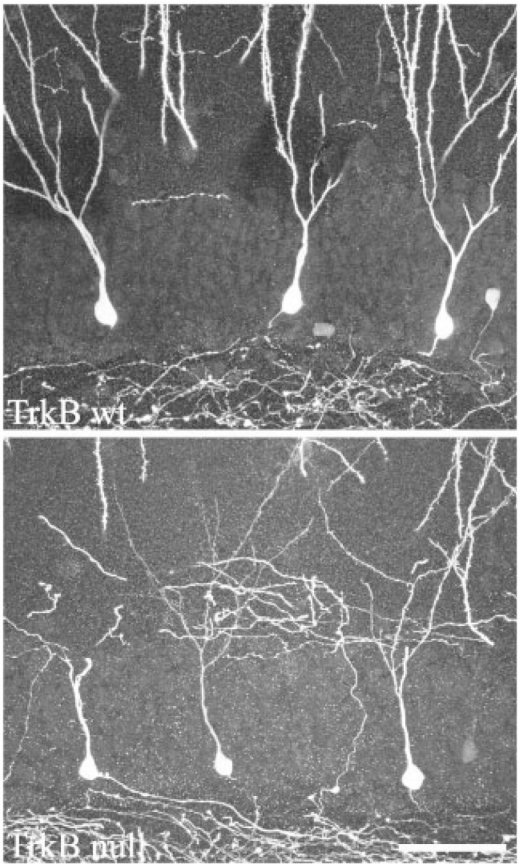

FIGURE 3.

GFP fills both the dendritic and axonal arbors of dentate granule cells in $TrkB^{+/+}$ and $TrkB^{-/-}$ mice crossed to Thy1 GFP-expressing mice. Images are confocal projections showing GFP-expressing dentate granule cells. All three cells in each image are located along the hilar border, and exhibit a single radially projecting dendrite as is typical for cells located in this region. Some dendrites are truncated at the surface of the tissue section in these images. Scale bar = 50 μm.

NIH-PA Author Manuscript

NIH-PA Author Manuscript

NIH-PA Author Manuscript

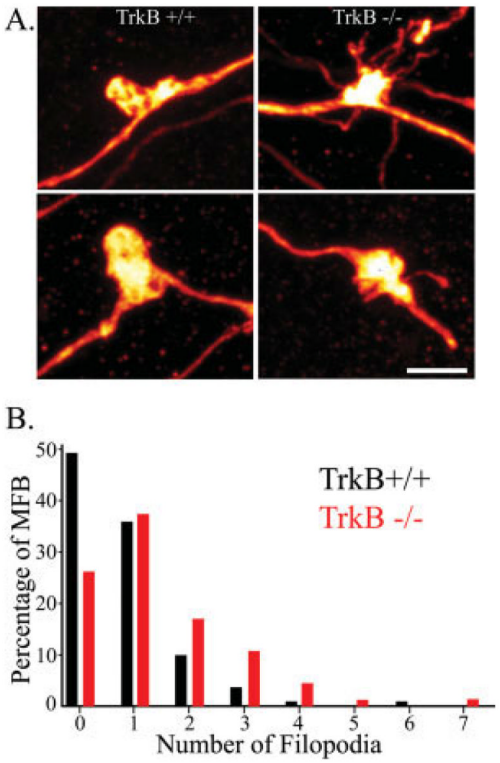

FIGURE 4.

A: Composite of confocal images showing dentate granule cell giant mossy fiber boutons. The number of filopodia arising from the giant boutons in TrkB$^{-/-}$ mice was significantly increased relative to TrkB$^{+/+}$ mice (*t*-test, $P = 0.006$). Scale bar = 3 μm. B: Frequency distribution showing the percentage of all mossy fiber boutons binned by the number of filopodia each possessed (minimum = 0; maximum = 7). Data from TrkB$^{+/+}$ is shown in black and data from TrkB$^{-/-}$ mice is shown in red. Note the prominent right shift in the percentage of boutons from TrkB$^{-/-}$ mice with greater numbers of filopodia. [Color figure can be viewed in the online issue, which is available at www.interscience.wiley.com.]

NIH-PA Author Manuscript

NIH-PA Author Manuscript

NIH-PA Author Manuscript

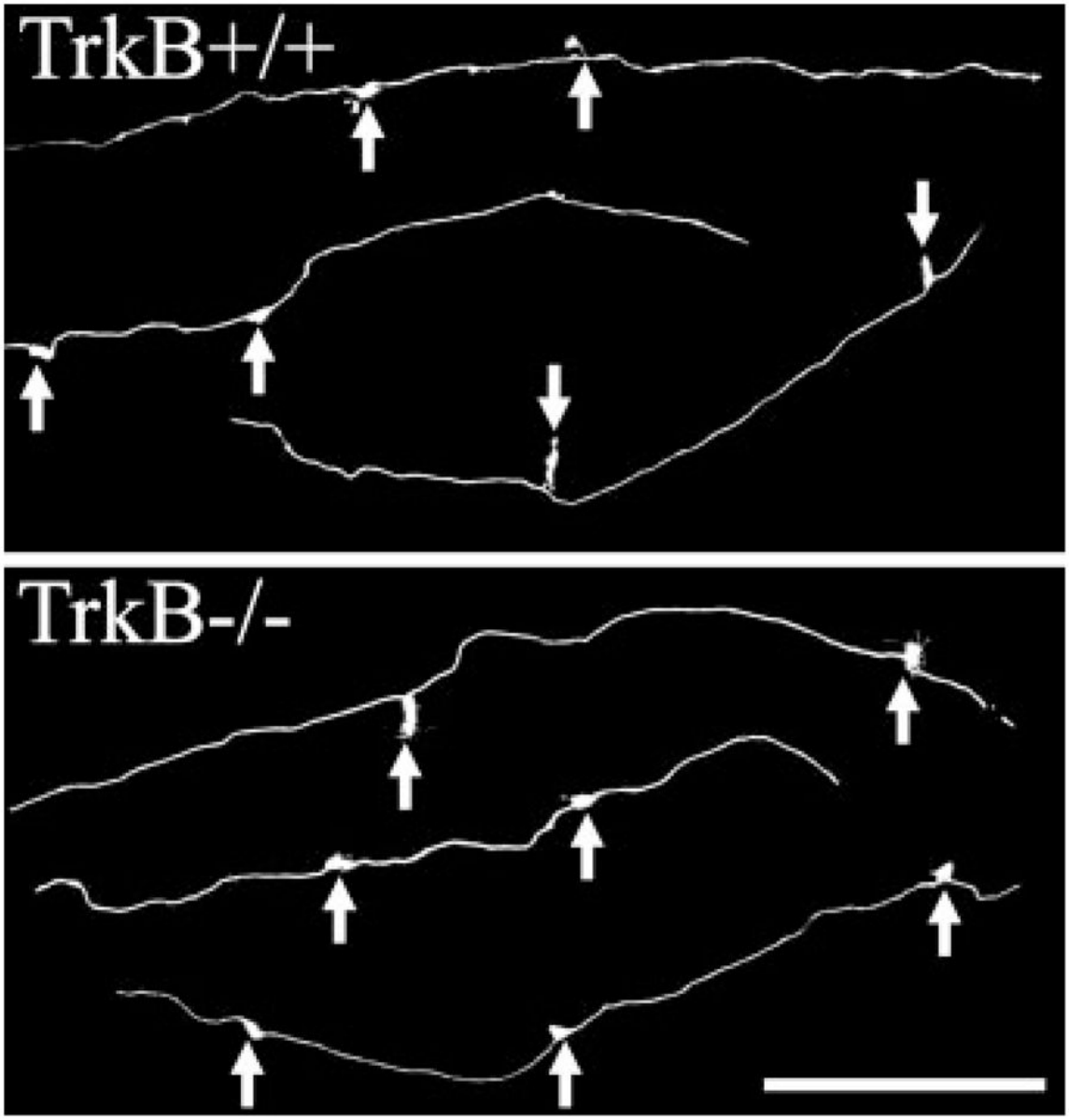

FIGURE 5.

Composite of confocal images showing lengths of mossy fiber axons with giant boutons denoted by arrows. The density of mossy fiber boutons along these axons did not differ between $TrkB^{-/-}$ and $TrkB^{+/+}$ mice. Images show mossy fiber axons in stratum lucidum of CA3b. Scale bar = 60 μm.

NIH-PA Author Manuscript

NIH-PA Author Manuscript

NIH-PA Author Manuscript

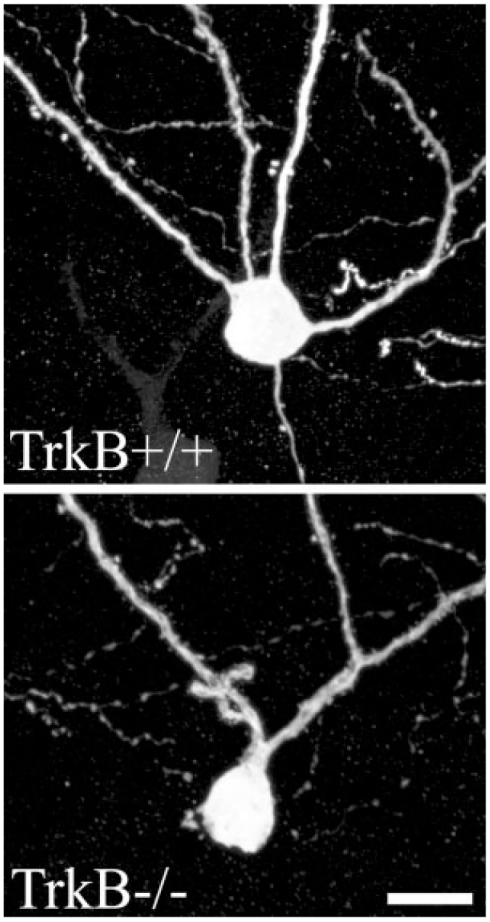

FIGURE 6.

Composite of confocal images showing dentate granule cell bodies and proximal dendrites. Dentate granule cell primary dendrite number was decreased in $TrkB^{-/-}$ mice relative to $TrkB^{+/+}$ littermates. Scale bar = 10 μm.

NIH-PA Author Manuscript

NIH-PA Author Manuscript

NIH-PA Author Manuscript

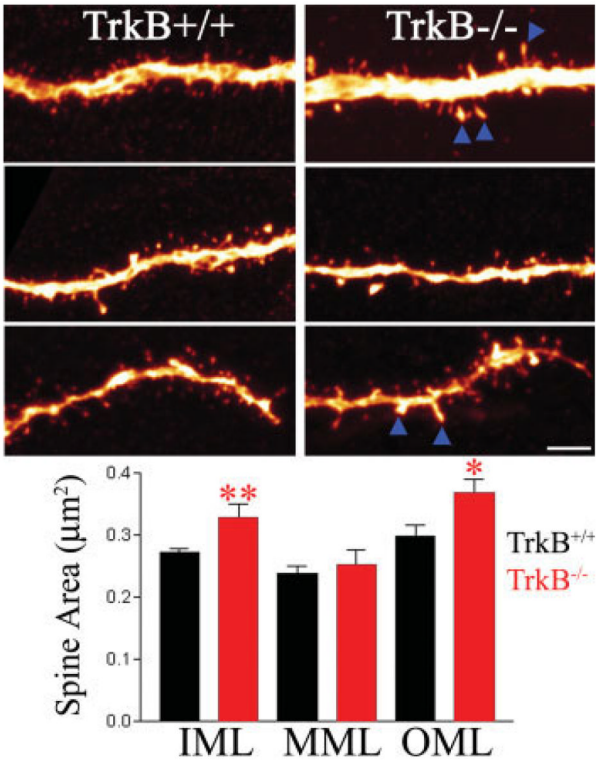

FIGURE 7.

Composite of confocal images showing dentate granule cell dendrites from the inner (top), middle (middle), and outer (bottom) molecular layers of $TrkB^{-/-}$ and $TrkB^{+/+}$ mice. Enlarged dendritic spines (arrowheads) were found along granule cell dendrites in the inner (IML) and outer molecular layers (OML). Spine profile area was not significantly increased in the middle molecular layer (MML). Scale bar = 3 μm. $*P < 0.05$. $**P < 0.01$. [Color figure can be viewed in the online issue, which is available at www.interscience.wiley.com.]